Report

A Dorsal SHH-Dependent Domain in the V-SVZ Produces Large Numbers of Oligodendroglial Lineage Cells in the Postnatal Brain

Cheuk Ka Tong,[1,4] Luis C. Fuentealba,[1,4] Jugal K. Shah,[1] Robert A. Lindquist,[1,2] Rebecca A. Ihrie,[3] Cristina D. Guinto,[1] Jose L. Rodas-Rodriguez,[1] and Arturo Alvarez-Buylla[1,2,*]

[1]Department of Neurological Surgery and The Eli and Edythe Broad Center of Regeneration Medicine and Stem Cell Research, University of California, San Francisco, San Francisco, CA 94143, USA
[2]Neuroscience Graduate Program, University of California, San Francisco, San Francisco, CA 94158, USA
[3]Departments of Cancer Biology and Neurological Surgery, Vanderbilt University Medical Center, Nashville, TN 37232-6840, USA
[4]Co-first author
*Correspondence: abuylla@stemcell.ucsf.edu
http://dx.doi.org/10.1016/j.stemcr.2015.08.013

SUMMARY

Neural stem cells in different locations of the postnatal mouse ventricular-subventricular zone (V-SVZ) generate different subtypes of olfactory bulb (OB) interneurons. High Sonic hedgehog (SHH) signaling in the ventral V-SVZ regulates the production of specific subtypes of neurons destined for the OB. Here we found a transient territory of high SHH signaling in the dorsal V-SVZ beneath the corpus callosum (CC). Using intersectional lineage tracing in neonates to label dorsal radial glial cells (RGCs) expressing the SHH target gene *Gli1*, we demonstrate that this region produces many CC cells in the oligodendroglial lineage and specific subtypes of neurons in the OB. The number of oligodendroglial cells generated correlated with the levels of SHH signaling. This work identifies a dorsal domain of SHH signaling, which is an important source of oligodendroglial cells for the postnatal mammalian forebrain.

INTRODUCTION

Oligodendrocyte progenitor cells (OPCs) in the mammalian cerebral cortex have been suggested to originate from the ventral telencephalon (He et al., 2001; Marshall and Goldman, 2002). However, cell fate mapping using *Emx1:: Cre* transgenic mice show that many oligodendrocytes in the cortex are generated dorsally (Gorski et al., 2002). These seemingly contradictory observations are reconciled in a study using *Nkx2.1::Cre; Gsh2::Cre* and *Emx1::Cre* transgenic mice to lineage trace progenitor cells of the medial and lateral ganglionic eminences (MGE and LGE) and the cortex, respectively. These analyses demonstrate three sequential waves of oligodendrocyte production in the forebrain (Kessaris et al., 2006). The first OPCs arise from the MGE and AEP in the ventral telencephalon at embryonic day 11.5 (E11.5); the second wave of OPCs originates from the LGE around E15, and the third wave comes from the cortex during the early postnatal period (Kessaris et al., 2006). The MGE and AEP are enriched with Sonic hedgehog (*Shh*), its receptor Patched (*Ptc*), and oligodendrocyte transcription factor 2 (*Olig2*) (Spassky et al., 2001; Tekki-Kessaris et al., 2001; Fuccillo et al., 2004). However, the region of origin of this third wave and whether these progenitors are regulated by SHH signaling remain unknown.

Interestingly, in rodents, the last wave of OPCs appears to be generated postnatally coinciding with the production of many neurons destined for the olfactory bulb (OB). These neurons and oligodendrocytes are derived from persistent germinal activity in the postnatal ventricular-subventricular zone (V-SVZ) (Levison and Goldman, 1993; Luskin and McDermott, 1994; Menn et al., 2006). The V-SVZ is an extensive germinal layer on the walls of the lateral ventricles that includes components derived from the MGE, LGE, septum, and cortex (Merkle et al., 2007; Alvarez-Buylla et al., 2008; Fuentealba et al., 2015). Different subregions of the V-SVZ are specialized for the production of different subtypes of OB interneurons, but the origin of OPCs from this postnatal germinal niche remains unknown. Here we identify a dorsal SHH-dependent domain in the postnatal V-SVZ, where many oligodendroglial lineage cells are generated. This domain may be critical for oligodendrogenesis and myelination in the postnatal forebrain.

RESULTS

Transient Expression of *Gli1* in the Dorsal V-SVZ

In the postnatal V-SVZ, SHH is important for the generation and proliferation of neural stem cells (Lai et al., 2003; Balordi and Fishell, 2007) and for the specification of regional identity (Ihrie et al., 2011; Merkle et al., 2014). Consistently, expression of *Gli1* is higher in the ventral V-SVZ compared with the dorsal V-SVZ (Fuccillo et al., 2004; Palma et al., 2005; Ihrie et al., 2011; Bai et al., 2002; Petrova et al., 2013). However, these studies were performed mainly on adult brains. In situ hybridization (ISH) for *Gli1* in mice at postnatal age (P)0, P7, P14, and P21 showed that *Gli1* expression at P0 and P7 was enriched not only at the anterior ventral (AV) V-SVZ
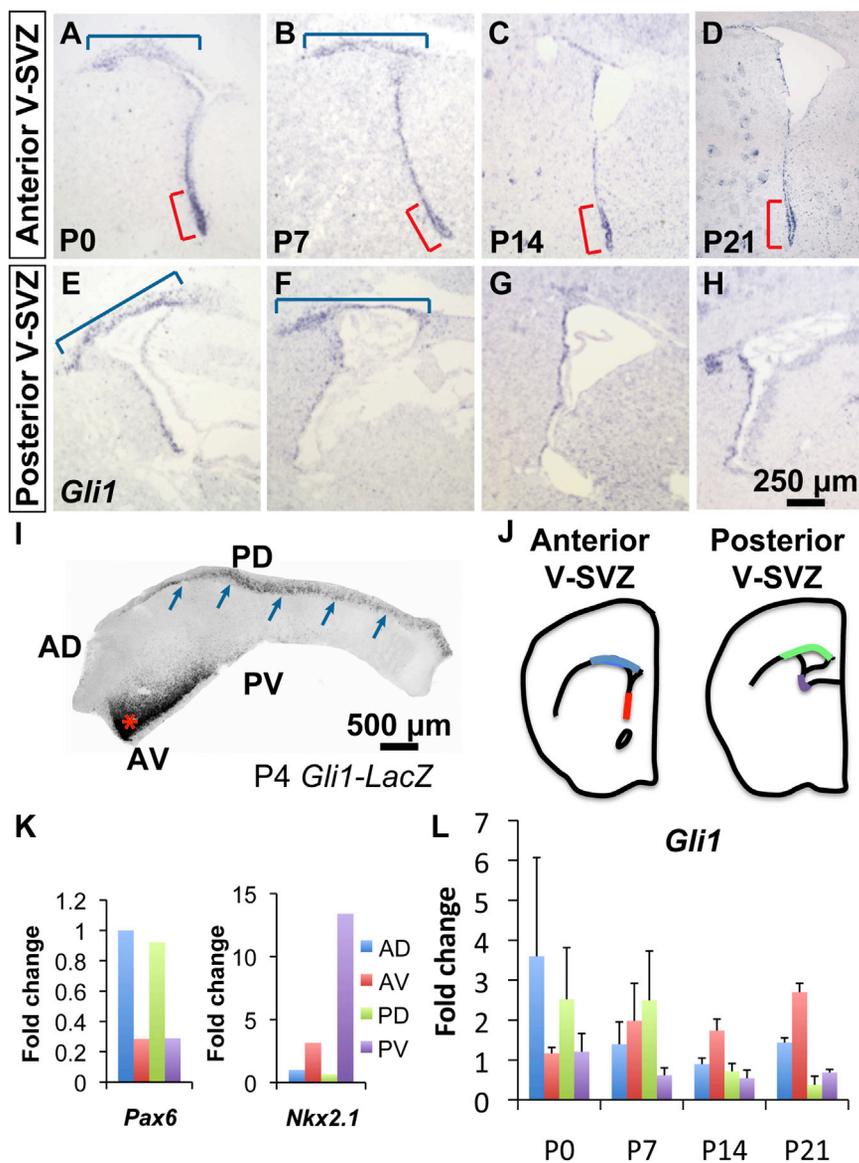
Figure 1. *Gli1* Expression Is Transiently Enriched in the Subcallosal Region

(A–H) ISH shows high expression of *Gli1* at the AV tip of the V-SVZ (red brackets). Low expression of *Gli1* is observed throughout the lateral walls of the lateral ventricle: anterior (A–D) and posterior (E–H) views are shown. At P0 and P7 (A, B, E, and F), *Gli1* expression is enriched in the subcallosal region (blue brackets); *Gli1* expression is reduced at P14 and P21 (C, D, G, and H).

(I) V-SVZ whole mount from P4 *Gli1-LacZ* mouse showing strong X-gal staining in the AV (red asterisk) and subcallosal domains (blue arrows).

(J) Schematic showing the AD (blue), AV (red), PD (green), and PV (purple) regions of the V-SVZ that were microdissected at P0, P7, P14, and P21.

(K and L) RT-PCR data from three animals per age group. A representative RT-PCR result confirming that *Pax6* is highly expressed in the dorsal regions whereas *Nkx2.1* is highly enriched in the ventral regions is shown (K). *Gli1* expression is enriched in both the dorsal regions and the AV V-SVZ at P0 and P7 but is decreased in the dorsal regions relative to the ventral regions at P14 and P21 (L).

The scale bar in (H) applies to (A)–(H) and represents 250 μm. The scale bar in (I) represents 500 μm.

(Figures 1A–1H), but also dorsally in a region between the lateral ventricle and the CC (the subcallosal V-SVZ) (Figures 1A, 1B, 1E, and 1F). Expression of *Gli1* in the subcallosal V-SVZ was reduced by P14 and mostly absent at P21 (Figures 1C, 1D, 1G, and 1H). In contrast, the ventral domain of high *Gli1* expression was maintained into adult life (Ihrie et al., 2011).

V-SVZ whole mounts (Mirzadeh et al., 2010) dissected from *Gli1::LacZ* reporter mice (Bai et al., 2002) at P4 clearly showed the two domains of *Gli1* expression (Figure 1I): in the AV region and at the dorsal edge of the whole mount corresponding to the subcallosal V-SVZ. qRT-PCR analysis of tissue dissected from the anterior dorsal (AD), AV, posterior dorsal (PD), and posterior ventral (PV) regions (Figure 1J) confirmed this temporal and spatial pattern of

expression. Expression of the transcription factors *Pax6* and *Nkx2.1*, which are highly expressed in the dorsal and ventral forebrain, respectively (Toresson et al., 2000; Xu et al., 2008), were used as controls for the microdissection (Figures 1J and 1K). At P0 and P7, elevated levels of *Gli1* were observed in the subcallosal V-SVZ (Figure 1L). However, at P14 and P21, the highest expression of *Gli1* was observed in the AV V-SVZ (Figure 1L). These results reveal a dorsal domain of elevated *Gli1* expression, which appears transiently during early postnatal development.

Radial Glia in the Subcallosal V-SVZ Produce Neurons and Oligodendroglial Cells

To determine the types of cells derived from the *Gli1*-expressing subcallosal V-SVZ, we injected adenovirus-expressing *Cre*
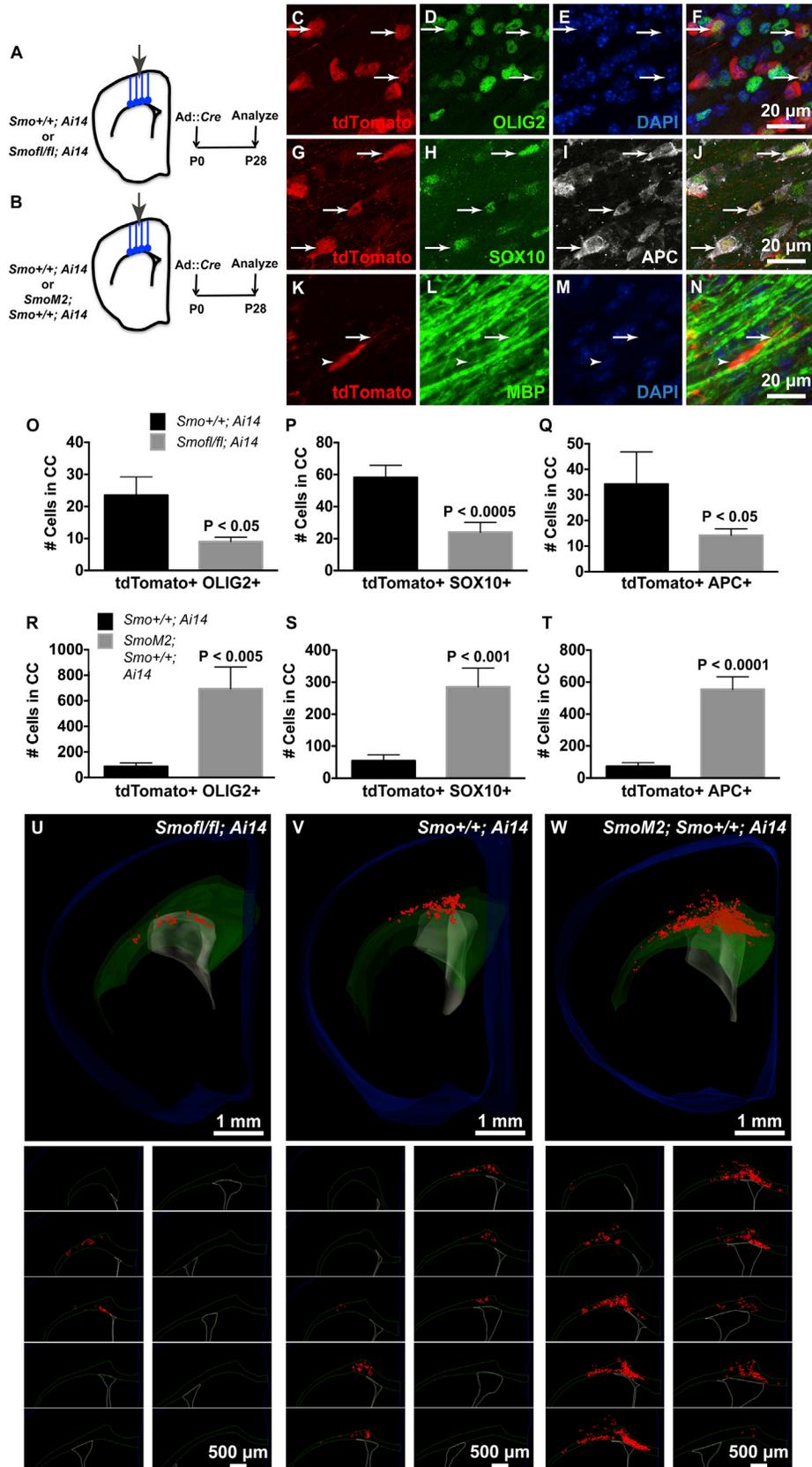
(Ad::*Cre*) next to the dorsal pia of neonatal *Ai14* reporter mice. This results in permanent labeling of radial glial cells (RGCs) through their basal processes in the cortex (Figures 2A and 2B) (Merkle et al., 2007). Analysis of the brains at P28 showed that, in addition to neurons in the OB, many tdTomato^{+} cells were present in the CC. These tdTomato^{+} cells expressed oligodendroglial lineage markers: OLIG2 (Figures 2C–2F), sex determining region Y-box 10 (SOX10), and adenomatous polyposis coli (APC) (Figures 2G–2J). Some tdTomato^{+} cells in the CC also had processes that contained the mature oligodendrocyte marker myelin basic protein (MBP) (Figures 2K–2N); however, these cells were rare, and it was difficult to colocalize the tdTomato signal, which was stronger in the cell body, with MBP staining, which were mainly in the processes. This suggests that subcallosal V-SVZ RGCs give rise to oligodendroglial cells that migrate to the CC postnatally.

Oligodendrogenesis at the Subcallosal V-SVZ Is SHH Dependent

Since the subcallosal V-SVZ transiently expressed the SHH target gene *Gli1* during early postnatal life (Figure 1), we next asked whether oligodendrogenesis in the subcallosal V-SVZ required SHH signaling. We injected Ad::*Cre* into *Smo^fl/fl*; *Ai14* mice (Long et al., 2001) at P0, to infect the RGCs at their cortical V-SVZ (Figure 2A). This allowed the labeling of cells derived from these RGCs, by the conditional activation of the *Ai14* reporter, and at the same time the conditional inactivation of *Smoothened* (*Smo*), which is essential for SHH signaling. Analysis of the brains at P28 showed more than 50% decrease in the tdTomato^{+} cells expressing OLIG2 (61.7%) (Figure 2O), SOX10 (59.5%) (Figure 2P), or APC (58.4%) (Figure 2Q) in the CC of the *Smo^fl/fl*; *Ai14* mice (Figure 2U) compared with the *Smo^+/+*; *Ai14* controls (Figure 2V). The opposite result was obtained when we injected Ad::*Cre* into *SmoM2; Smo^+/+*; *Ai14* mice (Figure 2B), which expressed a constitutively active form of the SMO receptor upon CRE recombination

(Jeong et al., 2004). An approximately 10-fold increase in the numbers of tdTomato[+] OLIG2^{+} (Figure 2R), tdTomato[+] SOX10^{+} (Figure 2S), and tdTomato[+] APC[+] (Figure 2T) cells was observed in the CC of *SmoM2; Smo^+/+*; *Ai14* mice (Figure 2W). These results indicate that oligodendrocyte production by subcallosal V-SVZ RGCs at P0 is regulated by SHH signaling; inactivation of *Smo* decreased, while constitutive activation of SMO (using *SmoM2*) increased the production of oligodendroglial cells.

Subcallosal V-SVZ *Gli1*-Expressing RGCs Produce Cells in the Oligodendrocyte Lineage

The above lineage tracing experiments show that large numbers of oligodendroglial cells are derived from subcallosal V-SVZ RGCs. To directly show that these oligodendrocytes are derived from those RGCs that express *Gli1*, we made use of *LacZ/EGFP* double reporter mice (Yamamoto et al., 2009), which express EGFP after dual CRE and FLP recombination (Figure 3A). By crossing these reporter mice with *Gli1::CreER* mice and administering tamoxifen to their offspring at P0–P2, we induced CRE recombination in the *Gli1*-expressing cells (Figure 3A). Then we stereotaxically injected adenovirus-expressing *Flp* (Ad::*Flp*) to target the RGCs at the cortical V-SVZ (Figure 3A). In this way, only the *Gli1*-expressing RGCs in the subcallosal V-SVZ and their progeny were labeled with EGFP.

As with the single dorsal targeting methods, the intersectional (CRE-FLP) genetic labeling resulted in EGFP^{+} neurons in the OB (Figure 3G) and many labeled cells in the CC (Figure 3B) at P28. The majority of EGFP^{+} cells in the CC corresponded to cells in the oligodendroglial lineage (Figure 3B). These cells expressed OLIG2 (Figure 3C), SOX10 (Figure 3D), and APC (Figure 3E). Some of the EGFP^{+} cells in the CC were fibrous astrocytes that expressed the glial fibrillary acidic protein (GFAP) (Figure 3F). Consistent with previous findings that RGCs in the dorsal V-SVZ generate superficial granule cells (sGCs) (Merkle et al., 2007), the majority of EGFP^{+} neurons in the OB

Figure 2. Inactivation and Ectopic Activation of SMO at the Cortical V-SVZ Lead to Decreased and Increased Oligodendrogenesis in the CC, Respectively

(A and B) Neonatal *Ai14* reporter mice were injected with Ad::*Cre* to infect RGCs in the cortical V-SVZ. In *Ai14* mice, tdTomato is expressed upon CRE recombination (Madisen et al., 2010).

(C–N) At P28, tdTomato^{+} cells in the CC expressed the oligodendroglial markers OLIG2 (C–F; arrows), SOX10, APC (G–J; arrows), and MBP (K–N; arrowheads, tdTomato[+] cell body; arrows, MBP[+] process).

(O–Q) Data from four animals per group. Compared with their *Smo^+/+*; *Ai14* littermates, *Smo^fl/fl*; *Ai14* mice have decreased tdTomato[+] OLIG2^{+} (O), tdTomato[+], SOX10^{+} (P), and tdTomato[+] APC[+] (Q) cells in the CC.

(R–T) Data from five animals per group. Ectopic activation of *SmoM2* results in increased cells expressing oligodendroglial markers in the CC.

(U–W) Neurolucida tracings. Compared to tdTomato^{+} cells in *Smo^+/+*; *Ai14* mice (V) and *Smo^fl/fl*; *Ai14* mice (U), *SmoM2; Smo^+/+*; *Ai14* mice have increased tdTomato^{+} cells in the CC (W).

Scale bars in (F), (J), and (N) apply to (C)–(N) and represent 20 μm. Scale bars in the large and small panels of (U), (V), and (W) represent 1 mm and 500 μm, respectively.

Sample #	Oligo (CC)	**Astro** (CC)	GC (OB)	PGC (OB)
1	13	2	17	2
2	108	11	262	12
3	15	4	17	0
4	13	2	13	0
5	20	7	30	2
% of total GFP + cells	37.5 ± 3.2	7.8 ± 1.7	52.2 ± 3.7	2.7 ± 1.1
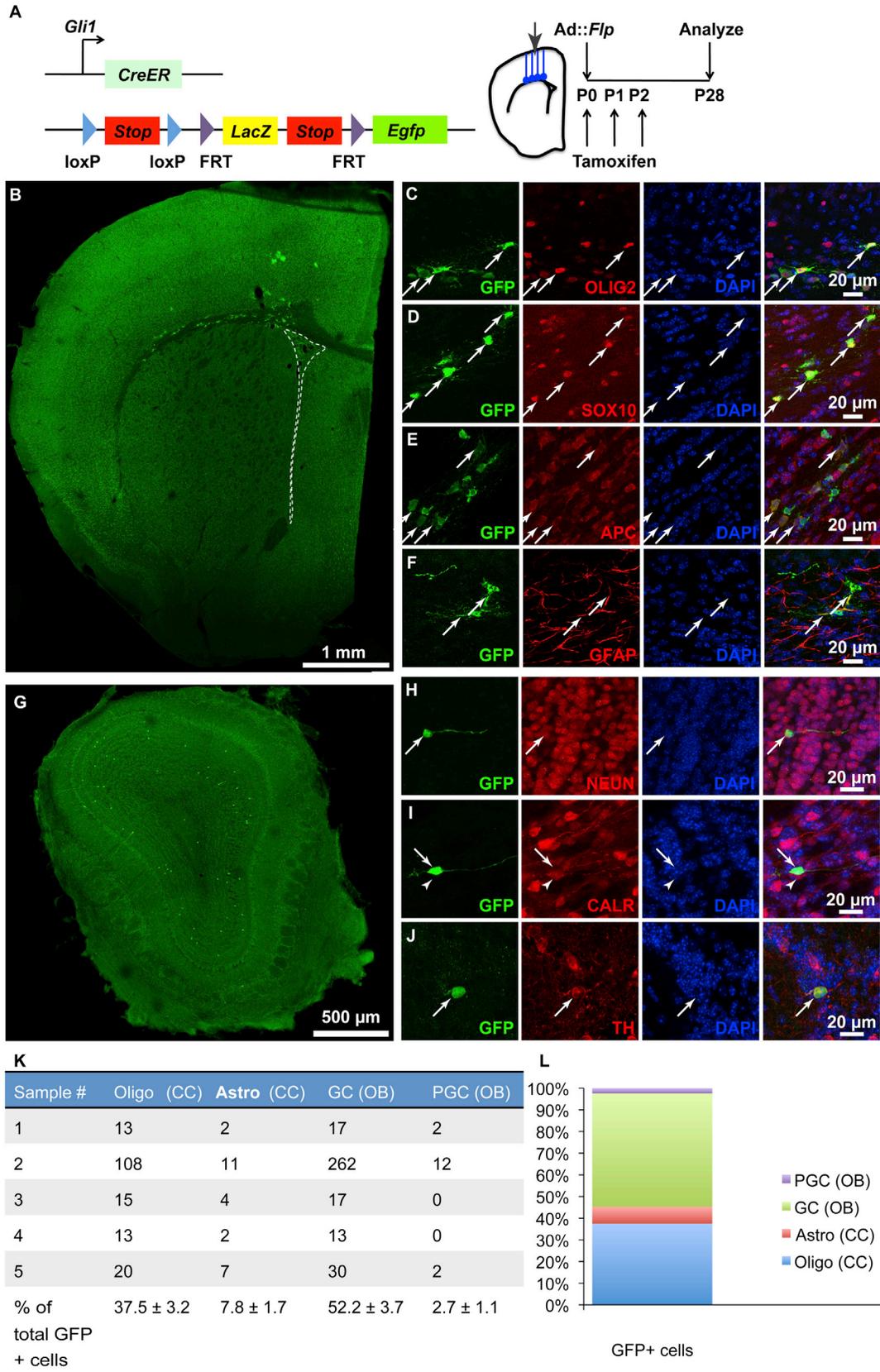
(legend on next page)

corresponded to sGCs (Figure 3G). These neurons expressed the pan-neuronal marker NEUN (Figure 3H) but did not express the calcium-binding protein calretinin (CALR) (Figure 3I). A small number of EGFP⁺ periglomerular cells (PGCs) expressed the dopaminergic neuronal marker tyrosine hydroxylase (TH) (Figure 3J). Of the EGFP⁺ cells, 37.5% ± 3.2% were oligodendroglial cells in the CC, 7.8% ± 1.7% were astrocytes in the CC, 52.2% ± 3.7% were OB GCs, and 2.7% ± 1.1% were PGCs (Figures 3K and 3L). A few EGFP⁺ cells were also present in the cortex (Figure 3B). These included SOX10⁺ oligodendroglial cells and protoplasmic astrocytes that were GFAP⁻ (data not shown). However, it is not clear whether these cortical cells were the progeny of Ad::Flp-infected RGCs or were directly infected by Ad::Flp along the needle track. These results show that Gli1-expressing, dorsally projecting RGCs give rise to a subpopulation of sGCs, PGCs, many CC oligodendroglial cells and a subpopulation of CC fibrous astrocytes.

Ectopic Activation of SMO Increases Oligodendrogenesis at the Dorso-lateral V-SVZ

The above experiments demonstrate that subcallosal V-SVZ RGCs produce many CC oligodendroglial cells and that this process is SHH dependent. In contrast, the dorso-lateral wall facing the striatum normally gives rise to very few oligodendrocytes in the CC (Menn et al., 2006). We were therefore curious whether activation of SHH signaling in the dorso-lateral V-SVZ had any effect on the production of oligodendrocytes. We performed SmoM2 activation by injecting Ad::Cre laterally into SmoM2; Smo⁺/⁺; Ai14 mice (Figure 4A). This resulted in a dramatic (10- to 20-fold) increase in the production of tdTomato⁺ cells (Figures 4E and 4F) that expressed OLIG2 (Figure 4B), SOX10 (Figure 4C), and APC (Figure 4D) in the CC. These observations suggest that as in the subcallosal V-SVZ, ectopic SHH activity in the dorso-lateral V-SVZ promotes the generation of oligodendroglial cells that migrate into the CC.

SHH Activity Increases Oligodendrogenesis at the Dorsal V-SVZ in the Adult

Our ISH (Figures 1C, 1D, 1G, and 1H) and RT-PCR (Figure 1L) data indicate that Gli1 expression in the subcallosal V-SVZ diminished after the first postnatal week. If SHH activity were reinstated in the adult, would dorsal V-SVZ progenitor cells be stimulated to produce oligodendrocytes? We injected Ad::GFAPpCre into the dorsal V-SVZ of P30 SmoM2; Smo⁺/⁺; Ai14 mice (Figure 4G). Analysis at 1 month post-injection showed a significantly (41.2%) higher number of tdTomato⁺ OLIG2⁺ cells in the CC of SmoM2; Smo⁺/⁺; Ai14 mice compared with Smo⁺/⁺; Ai14 mice (Figures 4H–4J). We also observed more tdTomato⁺ cells that expressed SOX10 and APC in the SmoM2; Smo⁺/⁺; Ai14 mice (Figures 4K–4R). This result suggests that ectopic activation of SMO in the dorsal V-SVZ promotes oligodendrogenesis in the adult. This is consistent with a previous study showing increased OPCs in the adult mouse CC upon SHH delivery in the lateral ventricle (Loulier et al., 2006).

DISCUSSION

We identified a dorsal V-SVZ domain that transiently expresses high levels of Gli1 during the first postnatal week in mice. We lineage traced Gli1-expressing RGCs in this dorsal domain and showed that a subpopulation of OB interneurons, CC astrocytes, and oligodendroglial cells are derived from this region. Genetic ablation of Smo in these dorsal V-SVZ RGCs resulted in a reduction in their production of oligodendroglial cells in the CC. In contrast, expression of constitutively active SmoM2 significantly increased the number of oligodendroglial cells produced. Moreover, this effect of SmoM2 was also observed in adult mice, when Gli1 expression was greatly diminished in the dorsal V-SVZ.

In the developing neural tube, levels of SHH ligand vary along the dorsoventral axis to create a morphogen gradient (Ahn and Joyner, 2004; Ribes and Briscoe,

---

Figure 3. *Gli1*-Expressing RGCs at the Cortical V-SVZ Give Rise to Oligodendroglial Cells in the CC

(A) Mice carrying *Gli1::CreER* and the *LacZ/EGFP* double reporter were given tamoxifen from P0–P2 and were injected with Ad::Flp at P0 to infect dorsal RGCs.

(B) At P28, GFP⁺ cells in the CC.

(C–F) Confocal micrographs of GFP⁺ cells in the CC expressing OLIG2 (C), SOX10 (D), APC (E), and GFAP (F).

(G) GFP⁺ sGCs and PGCs in the OB.

(H–J) Confocal micrographs showing a GFP⁺ NEUN⁺ GC (H), a GFP⁺ CALR⁻ GC (arrow in I), an adjacent GFP⁻ CALR⁺ GC (arrowhead in I) and a GFP⁺ TH⁺ PGC (J).

(K) Table showing numbers of GFP⁺ cells in the CC identified as oligodendroglia [Oligo(CC)] and astrocytes [astro(CC)] and cells in the OB identified as GCs [GC(OB)] and PGCs [PGC(OB)]. The last row shows the number of each cell type as a percentage of the total number of GFP⁺ cells.

(L) Graph showing percentage of each cell type in the GFP⁺ cells.

Data in (K) and (L) are from five animals. Scale bars represent 1 mm (B), 500 μm (G), and 20 μm (C–F and H–J).
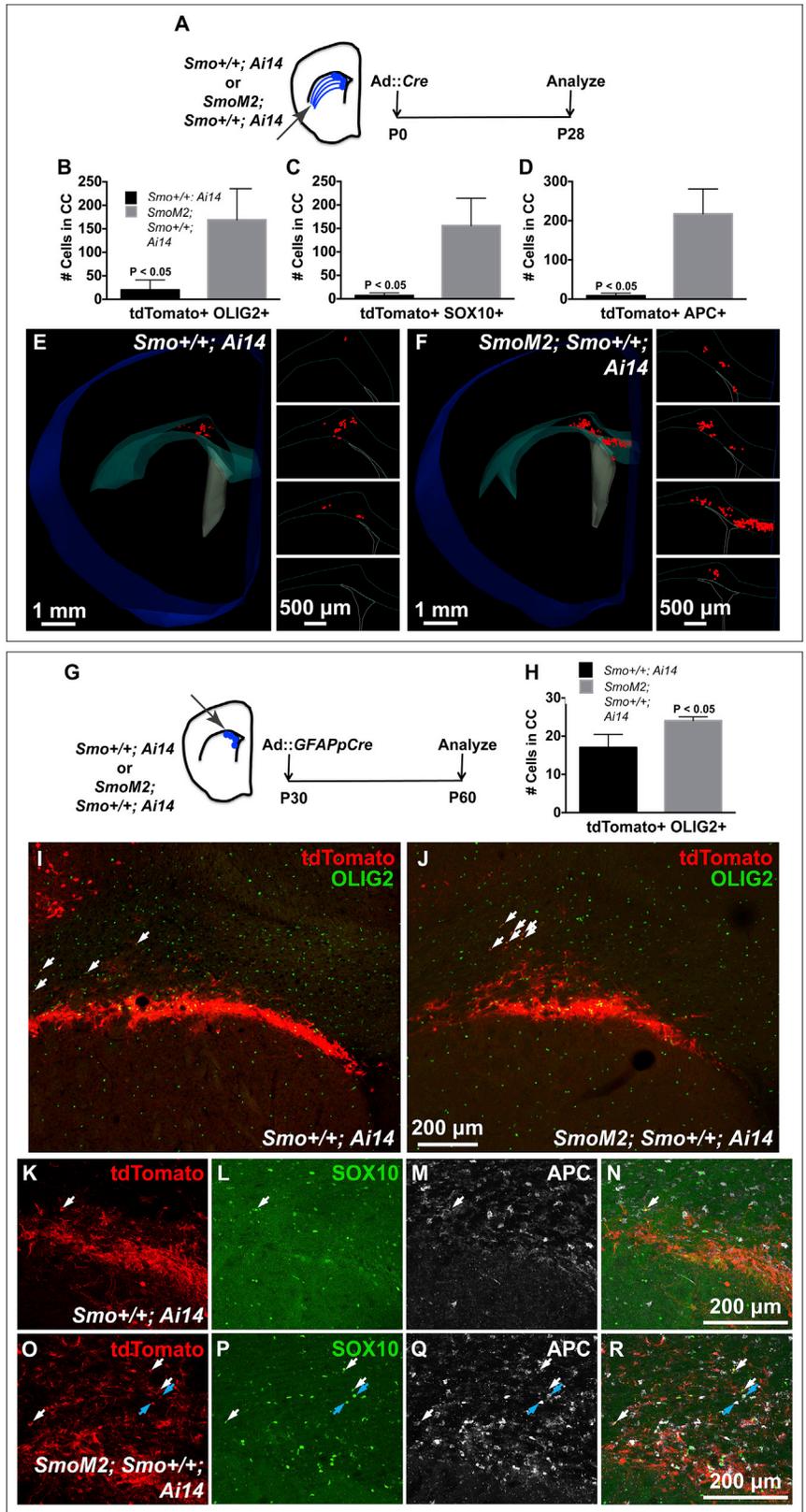
Figure 4. Activation of SMO in the Neonatal and Adult Dorso-lateral V-SVZ Results in Increased Oligodendroglial Cells in the CC

(A) Ad::*Cre* injected into the lateral striatum of neonatal pups infected RGCs at the dorso-lateral V-SVZ.

(B–D) At P28, the CC of *SmoM2; Smo$^{+/+}$; Ai14* mice have increased numbers of tdTomato$^+$ cells that expressed OLIG2 (B), SOX10 (C), and APC (D).

(E and F) Compared with the *Smo$^{+/+}$; Ai14* controls (E), *SmoM2; Smo$^{+/+}$; Ai14* mice (F) have increased tdTomato$^+$ cells in the CC; (Neurolucida tracings).

(G–J) Similarly, in the adult (P30) mice, activation of *SmoM2* in the dorsal V-SVZ B1 cells results in increased tdTomato$^+$ cells in the CC (G and I–J). Co-immunostaining shows higher number of tdTomato$^+$ OLIG2$^+$ cells in the *SmoM2; Smo$^{+/+}$; Ai14* mice (H–J). White arrows point to tdTomato$^+$ OLIG2$^+$ cells (I and J).

(K–R) Some tdTomato$^+$ cells in the CC also expressed SOX10 and/or APC. White arrows indicate tdTomato$^+$ SOX10$^+$ cells. Blue arrows indicate tdTomato$^+$ SOX10$^+$ APC$^+$ cells.

Data in (B–D) and (H) are from at least three animals per group. Scale bars in the large and small panels of (E) and (F) represent 1 mm and 500 μm, respectively. Scale bars in (I)–(R) represent 200 μm (I and J) and 200 μm (K–R).

2009), which results in graded levels of GLI. In the adult V-SVZ, we have previously reported that ablation of *Shh* decreases production of ventrally derived OB neuronal subtypes (Ihrie et al., 2011). In the present study, we identified a dorsal V-SVZ domain, where ectopic activation of the SHH pathway led not only to the respecification from superficial to deep interneurons (Ihrie et al., 2011), but also to a dramatic increase in oligodendrogenesis. In contrast, deletion of *Smo* had the opposite result (i.e., decreased oligodendrogenesis). Interestingly, dorsal-targeted inactivation of *Smo* also decreased production of dorsally derived neurons in the OB (data not shown). This observation indicates that SHH is not only controlling the types of neurons produced but also their numbers.

It is interesting that OB neurons produced from the transient *Gli1*-enriched subcallosal domain in juvenile mice mostly corresponded to sGCs, when they were derived from a region with active SHH signaling. It is possible that the relative levels of SHH signaling are adjusted in different domains. The intensity of *Gli1* expression (Figure 1) suggests higher levels ventrally than dorsally, but further quantitative analysis of SHH signaling would be required to understand how neuronal cell types are specified. Location in the V-SVZ might be associated not only with differences in SHH signaling levels, but also other signaling pathways. Similarly, high SHH signaling in V-SVZ progenitors is not always associated with high oligodendrogenesis; the ventral V-SVZ has high *Gli1* expression, but produces few oligodendrocytes postnatally (Kessaris et al., 2006; Menn et al., 2006).

These results reveal a dorsal domain in the juvenile telencephalon with high levels of SHH signaling, where many oligodendrocytes are produced. While our study provides evidence that this transient and restricted domain is an important source of OPCs, we cannot rule out that other regions within the *Emx1*^{+} dorsal forebrain (Kessaris et al., 2006) could also contribute to oligodendrogenesis. Together with other studies (Merkle et al., 2007, 2014), this work illustrates the high level of regionalization in the postnatal V-SVZ. It will be interesting to determine whether the developing human brain contains a similar *Gli1*-expressing territory. The production of large numbers of OPCs from a similar subcallosal territory could help explain the developmental origin of the many oligodendrocytes required for the greatly expanded white matter in the human brain. Gliomas can originate from OPCs (Alcantara Llaguno et al., 2009; Jacques et al., 2010; Liu et al., 2011); the territory of heightened OPC production we describe here could also help better understand the origin of some brain tumors.

EXPERIMENTAL PROCEDURES

Mice

All experiments were performed with adherence to the guidelines from the University of California, San Francisco Institutional Animal Care and Use Committee. Additional details are described in the Supplemental Experimental Procedures.

V-SVZ Whole-Mount Preparation

V-SVZ whole-mount dissection was carried out as previously described (Mirzadeh et al., 2010). X-gal staining was performed after 30-min fixation in 4% paraformaldehyde (PFA).

ISH

ISH was performed in 12-μm sections using standard procedures (Han et al., 2008; Ihrie et al., 2011) and antisense riboprobe from *Gli1* cDNA (from A. Ruiz I Altaba, University of Geneva Medical School).

qRT-PCR

Different regions of the V-SVZ (Figure 1J) were microdissected from 300-μm vibratome sections of unfixed brains for RT-PCR analysis. Additional details are described in the Supplemental Experimental Procedures.

Immunohistochemistry

Fifty-μm tissue sections were incubated with primary antibodies (Abs) at 4°C overnight, followed by secondary Abs at 4°C overnight. Additional details are described in the Supplemental Experimental Procedures.

Virus Injections

Neonatal pups were injected with 20 nl adenovirus in a region-specific manner as previously described (Merkle et al., 2007). Adult (P30) mice were injected with 20 nl Ad::*GFAPpCre* as previously described (Merkle et al., 2007). Additional details are described in the Supplemental Experimental Procedures.

SUPPLEMENTAL INFORMATION

Supplemental Information includes Supplemental Experimental Procedures and can be found with this article online at http://dx.doi.org/10.1016/j.stemcr.2015.08.013.

REFERENCES

Ahn, S., and Joyner, A.L. (2004). Dynamic changes in the response of cells to positive hedgehog signaling during mouse limb patterning. Cell *118*, 505–516.

Alcantara Llaguno, S., Chen, J., Kwon, C.H., Jackson, E.L., Li, Y., Burns, D.K., Alvarez-Buylla, A., and Parada, L.F. (2009). Malignant astrocytomas originate from neural stem/progenitor cells in a somatic tumor suppressor mouse model. Cancer Cell *15*, 45–56.

Alvarez-Buylla, A., Kohwi, M., Nguyen, T.M., and Merkle, F.T. (2008). The heterogeneity of adult neural stem cells and the emerging complexity of their niche. Cold Spring Harb. Symp. Quant. Biol. *73*, 357–365.

Bai, C.B., Auerbach, W., Lee, J.S., Stephen, D., and Joyner, A.L. (2002). Gli2, but not Gli1, is required for initial Shh signaling and ectopic activation of the Shh pathway. Development *129*, 4753–4761.

Balordi, F., and Fishell, G. (2007). Mosaic removal of hedgehog signaling in the adult SVZ reveals that the residual wild-type stem cells have a limited capacity for self-renewal. J. Neurosci. *27*, 14248–14259.

Fuccillo, M., Rallu, M., McMahon, A.P., and Fishell, G. (2004). Temporal requirement for hedgehog signaling in ventral telencephalic patterning. Development *131*, 5031–5040.

Fuentealba, L.C., Rompani, S.B., Parraguez, J.I., Obernier, K., Romero, R., Cepko, C.L., and Alvarez-Buylla, A. (2015). Embryonic origin of postnatal neural stem cells. Cell *161*, 1644–1655.

Gorski, J.A., Talley, T., Qiu, M., Puelles, L., Rubenstein, J.L., and Jones, K.R. (2002). Cortical excitatory neurons and glia, but not GABAergic neurons, are produced in the Emx1-expressing lineage. J. Neurosci. *22*, 6309–6314.

Han, Y.G., Spassky, N., Romaguera-Ros, M., Garcia-Verdugo, J.M., Aguilar, A., Schneider-Maunoury, S., and Alvarez-Buylla, A. (2008). Hedgehog signaling and primary cilia are required for the formation of adult neural stem cells. Nat. Neurosci. *11*, 277–284.

He, W., Ingraham, C., Rising, L., Goderie, S., and Temple, S. (2001). Multipotent stem cells from the mouse basal forebrain contribute GABAergic neurons and oligodendrocytes to the cerebral cortex during embryogenesis. J. Neurosci. *21*, 8854–8862.

Ihrie, R.A., Shah, J.K., Harwell, C.C., Levine, J.H., Guinto, C.D., Lezameta, M., Kriegstein, A.R., and Alvarez-Buylla, A. (2011). Persistent sonic hedgehog signaling in adult brain determines neural stem cell positional identity. Neuron *71*, 250–262.

Jacques, T.S., Swales, A., Brzozowski, M.J., Henriquez, N.V., Linehan, J.M., Mirzadeh, Z., O' Malley, C., Naumann, H., Alvarez-Buylla, A., and Brandner, S. (2010). Combinations of genetic mutations in the adult neural stem cell compartment determine brain tumour phenotypes. EMBO J. *29*, 222–235.

Jeong, J., Mao, J., Tenzen, T., Kottmann, A.H., and McMahon, A.P. (2004). Hedgehog signaling in the neural crest cells regulates the patterning and growth of facial primordia. Genes Dev. *18*, 937–951.

Kessaris, N., Fogarty, M., Iannarelli, P., Grist, M., Wegner, M., and Richardson, W.D. (2006). Competing waves of oligodendrocytes in the forebrain and postnatal elimination of an embryonic lineage. Nat. Neurosci. *9*, 173–179.

Lai, K., Kaspar, B.K., Gage, F.H., and Schaffer, D.V. (2003). Sonic hedgehog regulates adult neural progenitor proliferation in vitro and in vivo. Nat. Neurosci. *6*, 21–27.

Levison, S.W., and Goldman, J.E. (1993). Both oligodendrocytes and astrocytes develop from progenitors in the subventricular zone of postnatal rat forebrain. Neuron *10*, 201–212.

Liu, C., Sage, J.C., Miller, M.R., Verhaak, R.G., Hippenmeyer, S., Vogel, H., Foreman, O., Bronson, R.T., Nishiyama, A., Luo, L., and Zong, H. (2011). Mosaic analysis with double markers reveals tumor cell of origin in glioma. Cell *146*, 209–221.

Long, F., Zhang, X.M., Karp, S., Yang, Y., and McMahon, A.P. (2001). Genetic manipulation of hedgehog signaling in the endochondral skeleton reveals a direct role in the regulation of chondrocyte proliferation. Development *128*, 5099–5108.

Loulier, K., Ruat, M., and Traiffort, E. (2006). Increase of proliferating oligodendroglial progenitors in the adult mouse brain upon Sonic hedgehog delivery in the lateral ventricle. J. Neurochem. *98*, 530–542.

Luskin, M.B., and McDermott, K. (1994). Divergent lineages for oligodendrocytes and astrocytes originating in the neonatal forebrain subventricular zone. Glia *11*, 211–226.

Madisen, L., Zwingman, T.A., Sunkin, S.M., Oh, S.W., Zariwala, H.A., Gu, H., Ng, L.L., Palmiter, R.D., Hawrylycz, M.J., Jones, A.R., et al. (2010). A robust and high-throughput Cre reporting and characterization system for the whole mouse brain. Nat. Neurosci. *13*, 133–140.

Marshall, C.A., and Goldman, J.E. (2002). Subpallial dlx2-expressing cells give rise to astrocytes and oligodendrocytes in the cerebral cortex and white matter. J. Neurosci. *22*, 9821–9830.

Menn, B., García-Verdugo, J.M., Yaschine, C., Gonzalez-Perez, O., Rowitch, D., and Alvarez-Buylla, A. (2006). Origin of oligodendrocytes in the subventricular zone of the adult brain. J. Neurosci. *26*, 7907–7918.

Merkle, F.T., Mirzadeh, Z., and Alvarez-Buylla, A. (2007). Mosaic organization of neural stem cells in the adult brain. Science *317*, 381–384.

Merkle, F.T., Fuentealba, L.C., Sanders, T.A., Magno, L., Kessaris, N., and Alvarez-Buylla, A. (2014). Adult neural stem cells in distinct microdomains generate previously unknown interneuron types. Nat. Neurosci. *17*, 207–214.

Mirzadeh, Z., Doetsch, F., Sawamoto, K., Wichterle, H., and Alvarez-Buylla, A. (2010). The subventricular zone en-face: whole-mount staining and ependymal flow. J. Vis. Exp. *39*, 1938.

Palma, V., Lim, D.A., Dahmane, N., Sánchez, P., Brionne, T.C., Herzberg, C.D., Gitton, Y., Carleton, A., Alvarez-Buylla, A., and Ruiz i Altaba, A. (2005). Sonic hedgehog controls stem cell behavior in the postnatal and adult brain. Development *132*, 335–344.

Petrova, R., Garcia, A.D., and Joyner, A.L. (2013). Titration of GLI3 repressor activity by sonic hedgehog signaling is critical for maintaining multiple adult neural stem cell and astrocyte functions. J. Neurosci. *33*, 17490–17505.

Ribes, V., and Briscoe, J. (2009). Establishing and interpreting graded Sonic Hedgehog signaling during vertebrate neural tube patterning: the role of negative feedback. Cold Spring Harb. Perspect. Biol. *1*, a002014.

Spassky, N., Heydon, K., Mangatal, A., Jankovski, A., Olivier, C., Queraud-Lesaux, F., Goujet-Zalc, C., Thomas, J.L., and Zalc, B. (2001). Sonic hedgehog-dependent emergence of oligodendrocytes in the telencephalon: evidence for a source of oligodendrocytes in the olfactory bulb that is independent of PDGFRalpha signaling. Development *128*, 4993–5004.

Tekki-Kessaris, N., Woodruff, R., Hall, A.C., Gaffield, W., Kimura, S., Stiles, C.D., Rowitch, D.H., and Richardson, W.D. (2001). Hedgehog-dependent oligodendrocyte lineage specification in the telencephalon. Development *128*, 2545–2554.

Toresson, H., Potter, S.S., and Campbell, K. (2000). Genetic control of dorsal-ventral identity in the telencephalon: opposing roles for Pax6 and Gsh2. Development *127*, 4361–4371.

Xu, Q., Tam, M., and Anderson, S.A. (2008). Fate mapping Nkx2.1-lineage cells in the mouse telencephalon. J. Comp. Neurol. *506*, 16–29.

Yamamoto, M., Shook, N.A., Kanisicak, O., Yamamoto, S., Wosczyna, M.N., Camp, J.R., and Goldhamer, D.J. (2009). A multifunctional reporter mouse line for Cre- and FLP-dependent lineage analysis. Genesis *47*, 107–114.